Journal of Sound and Vibration ■ (■■■■) ■■■–■■■

Contents lists available at ScienceDirect

Journal of Sound and Vibration

journal homepage: www.elsevier.com/locate/jsvi

Experimental characterization of a nonlinear vibration absorber using free vibration

Bin Tang [a,*], M.J. Brennan [b], G. Gatti [c], N.S. Ferguson [d]

[a] Institute of Internal Combustion Engine, Dalian University of Technology, Dalian 116023, China
[b] Departamento de Engenharia Mecânica, UNESP Ilha Solteira, SP 15385-000, Brasil
[c] Department of Mechanical, Energy and Management Engineering, University of Calabria, Arcavacata di Rende, 87036 Cosenza, Italy
[d] Institue of of Sound and Vibration Research, University of Southampton, Southampton SO17 1BJ, UK

ARTICLE INFO

Article history:
Received 20 January 2015
Received in revised form
13 November 2015
Accepted 18 December 2015
Handling Editor: L.N. Virgin

Keywords:
Nonlinear vibration absorber
Free vibration
Cubic stiffness
Envelope
Instantaneous damped natural frequency

ABSTRACT

Knowledge of the nonlinear characteristics of a vibration absorber is important if its performance is to be predicted accurately when connected to a host structure. This can be achieved theoretically, but experimental validation is necessary to verify the modelling procedure and assumptions. This paper describes the characterization of such an absorber using a novel experimental procedure. The estimation method is based on a free vibration test, which is appropriate for a lightly damped device. The nonlinear absorber is attached to shaker which is operated such that the shaker works in its mass-controlled regime, which means that the shaker dynamics, which are also included in the measurement, are considerably simplified, which facilitates a simple estimation of the absorber properties. From the free vibration time history, the instantaneous amplitude and instantaneous damped natural frequency are estimated using the Hilbert transform. The stiffness and damping of the nonlinear vibration absorber are then estimated from these quantities. The results are compared with an analytical solution for the free vibration of the nonlinear system with cubic stiffness and viscous damping, which is also derived in the paper using an alternative approach to the conventional perturbation methods. To further verify the approach, the results are compared with a method in which the internal forces are balanced at each measured instant in time.

1. Introduction

The vibration absorber has become a well-established vibration control measure since the first patent on the device by Frahm [1] and the subsequent detailed analysis by Ormondroyd and Den Hartog in 1928 [2]. Since then there has been a substantial body of work on various types of absorbers, most of which are described in a series of review papers [3–6]. This paper is concerned with a specific type of nonlinear absorber in which the stiffness of the device is a function of the excitation level. Roberson [7] was one of the first to discuss this type of absorber in an article where he considered the effects of both softening and hardening springs in the device. Following this concept, several other researchers have reported various aspects of nonlinear absorbers, for example [8–13]. Recently, Zhu et al. [14] investigated the performance of a nonlinear absorber, which has both nonlinear damping and nonlinear stiffness. A recent area of research has involved

* Corresponding author. Tel.: +86 411 84709803; fax: +86 411 84708460.
E-mail address: btang@dlut.edu.cn (B. Tang).

http://dx.doi.org/10.1016/j.jsv.2015.12.040
0022-460X/

replacing the absorber stiffness with a purely nonlinear stiffness. This was pioneered by Vakakis et al. [15], who showed that energy could be efficiently transferred from the host structure to the absorber – the so-called targeted energy transfer approach. Specific tuning approaches for nonlinear absorbers have been discussed by Viguié and Kerschen [16], and Brennan and Gatti [17].

There has been a vast research effort on nonlinear vibration absorbers, and the literature cited above is only a fraction of that reported. There is, however, a scarcity of papers on the experimental characterization of such devices. This is the primary motivation of the work reported here. There is extensive literature on nonlinear system identification, and a comprehensive review on this topic has been provided by Kerschen et al. [18]. Of particular interest is the method which involves free vibration in which only a measurement of the response is necessary. This is highly appropriate for a lightly damped nonlinear absorber with a hardening stiffness nonlinearity discussed in this paper. The method involves the excitation of the absorber by a shaker, which is driven at a single frequency close to the jump-down frequency, and then switched off [19,20], so that the absorber mass vibrates freely. This approach had been taken many years earlier by Parzygnat and Pao [21,22], who studied the transient response during nonlinear jumps of a clamped circular plate, both analytically and experimentally. However, since the 1970s, there have been significant advances in both instrumentation and signal processing on digitized time histories and this facilitates the approach taken in this paper, which closely follows the procedures in [19,20].

The basic idea is to measure the backbone curve and the decay of free vibration then to relate these to the system parameters as described by Benhafsi et al. [23]. An approach related to this method in which the backbone curve is estimated from the jump-down frequencies has been recently reported by some of the authors of this paper [24]. A nonlinear vibration absorber, used in the thesis by Hsu [25], is tested in a particular configuration with an electrodynamic shaker, such that the dynamics of the shaker are largely decoupled from the dynamics of the absorber. The results are compared with an analytical solution for the free vibration of the nonlinear absorber, which is also derived using an alternative approach to the conventional perturbation methods. To further verify the approach, the results are compared with those determined from the Restoring Force Surface (RFS) method [26].

2. Nonlinear vibration absorber and the measured free vibration

2.1. Description of the device

The nonlinear vibration absorber is shown in Fig. 1. It consists of a 7.5 g mass attached to a thin circular brass plate of 0.15 mm thickness and 52 mm diameter, and is described in detail in Ref. [25]. The brass plate is sandwiched between two aluminium rings which provide a clamped boundary. The vibration is in the vertical direction as shown in Fig. 1(a). If the absorber vibrates with a low level, the dominant stiffness is from bending of the plate, and the system behaves linearly. However, as the vibration level increases, the in-plane stretching of the plate contributes to the stiffness resulting in a hardening nonlinear stiffness. Thus the nonlinear absorber is expected to behave predominantly as a hardening Duffing oscillator with linear damping [27].

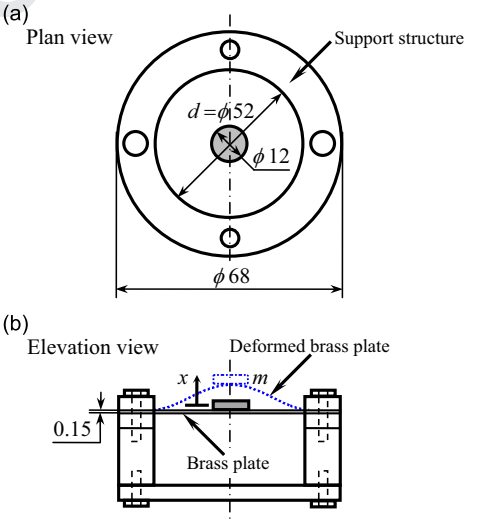

Fig. 1. Drawing of the nonlinear vibration absorber. (a) plan view and (b) elevation view. x is the displacement response of the mass; material propeties of the thin circular brass plate are: density $\rho \approx 8500$ kg/m^3, and Young's modulus $E \approx 110$ GPa. (All scales of the structure are in mm.)

Please cite this article as: B. Tang, et al., Experimental characterization of a nonlinear vibration absorber using free vibration, *Journal of Sound and Vibration* (2016), http://dx.doi.org/10.1016/j.jsv.2015.12.040

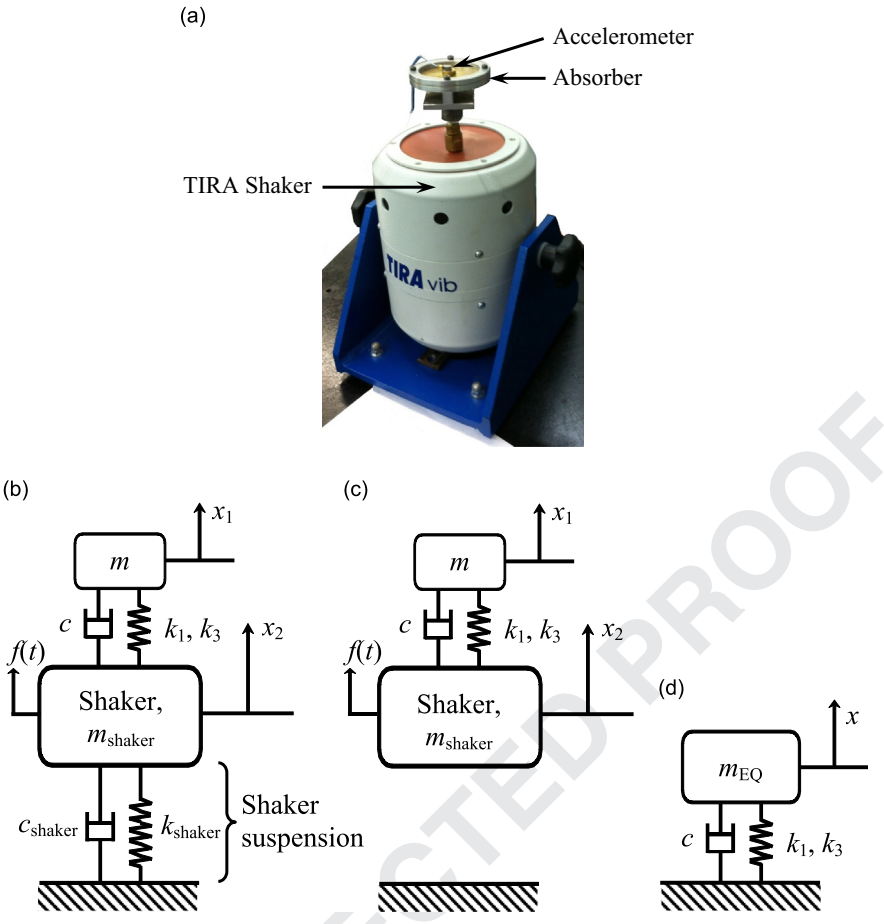

Fig. 2. Experimental set-up for the free vibration test. (a) photo of the test-rig, (b) model of the test-rig, (c) simplified model with the shaker, and (d) simplified model.

2.2. Description of the experimental test rig

To determine the stiffness and damping properties of the absorber, it is necessary to measure the relative displacement between the clamped boundary and the absorber mass in the centre of the plate. Free vibration is of interest in this paper, and to excite the absorber so that it vibrates freely, it can either be firmly attached to the ground and an impact force applied, or it can be attached to a shaker, excited close to its jump-down frequency and then the shaker switched-off [19]. In the latter case, provided that the motion of the shaker is small compared to the motion of the absorber mass, then the absolute motion of this mass is approximately equal to the relative motion between the mass and the support structure. As the shaker method offers much more control, it was used to excite the absorber. It should be emphasized, however, that this approach needs to be used with care because the shaker dynamics have to be considered, and this is further discussed below.

A photograph of the absorber attached to the shaker (TIRA TV51120) is shown in Fig. 2(a), and a lumped-parameter model of this set-up is shown in Fig. 2(b). The armature of the electro-dynamic shaker and support frame can be modelled as a mass m_{shaker}. The suspension system of the shaker can be modelled as a parallel combination of a linear damper c_{shaker}, and a linear spring k_{shaker}. Attached to this is the vibration absorber consisting of a small mass m, linear damper c, linear stiffness k_1, and cubic nonlinear stiffness k_3. The experimental set-up was designed so that the linear natural frequency corresponding to the first mode of vibration and the corresponding jump-down frequency of the attached structure were much higher than the natural frequency of the shaker. It was specifically configured in this way so that the shaker would behave simply as a mass from the dynamic point of view for the free vibration test. Thus, the suspension had a negligible effect on the free vibration and could be discarded in subsequent analysis of the data. The test rig was therefore much simpler than that in Refs. [21,22]. The simplification model of the test-rig can be justified by the following reasoning. The frequency at which the absorber vibrates freely in its first mode (which is about 90 Hz) is well above the natural frequency of the shaker, (which is about 35 Hz). The excitation force applied to the shaker mass at 90 Hz splits approximately three ways; to the force associated with the shaker mass, the shaker damping and the shaker stiffness in the respective ratio of 6.6:0.15:1, and this is obtained by considering the actual shaker parameters as estimated below and reported in Table 1.

Please cite this article as: B. Tang, et al., Experimental characterization of a nonlinear vibration absorber using free vibration, *Journal of Sound and Vibration* (2016), http://dx.doi.org/10.1016/j.jsv.2015.12.040

Thus, at an excitation frequency of 90 Hz, the stiffness and damping of the shaker can be neglected, which results in the equivalent system shown in Fig. 2(c). Now, for low displacement levels where the nonlinear stiffness force is very small compared to the linear stiffness force, the natural frequency of the system shown in Fig. 2(c) is given by $\omega_n = \sqrt{k_1/m_{EQ}}$, where $m_{EQ} = m_{shaker}m/(m_{shaker}+m)$. Further, if the mass of the absorber (which was 7.55 g) is much less than the mass of the shaker (which was 351 g) so that $m \ll m_{shaker}$ then $x_1 \gg x_2$ and the free-vibration of the absorber can be modelled by the system shown in Fig. 2(d), in which $x \approx x_1$. Because the system was designed in this specific way, the shaker dynamics are considerably simplified, and the resulting absorber-shaker system behaves predominantly as a single-degree-of-freedom system facilitating a relatively straight-forward determination of the stiffness and damping of the absorber from the time history of free vibration of the absorber mass. Note, that it is assumed that any damping due to the accelerometer cable is negligible compared to that due to the absorber.

2.3. Experimental procedure and results

Using an Agilent 33500B signal generator to supply the shaker through a TIRA BAA 500 power amplifier, a slow frequency sweep from low to high frequency was carried out to determine the jump-down frequency of the system. It was found to be about 149 Hz. The system was then excited at 148 Hz, with the power amplifier in current mode (to ensure that it added no damping to the system), and allowed to reach steady-state. The signal generator was then switched off so that the system vibration freely decayed away. The transient time domain signal was measured using a PCB 352A25 accelerometer attached to the mass as shown in Fig. 1, and captured using an Agilent DSO7034B Digital Storage Oscilloscope. The acceleration time history was then passed through a band-pass filter with cut-off frequencies of 50 Hz and 250 Hz, and then numerically integrated twice with respect to time to give the displacement response. This is shown in Fig. 3. The time periods over which there was steady-state and free vibration (transient) are marked in the figure. It should also be noted that when the source signal was switched off there is a small time period where the movement of the shaker was not as the transient model predicts, which is marked as a critical state (CS) in Fig. 3.

If the displacement response of the mass is given by $x(t)$, then the complex analytic time signal can be written as [19–20]

$$w(t) = x(t) + jH[x(t)] \tag{1}$$

where $H[x(t)]$ is the Hilbert transform of the displacement time history. Using the Hilbert transform [19–20], the envelope $A(t) = |w(t)|$ and instantaneous phase $\phi(t) = \arctan[H[x(t)]/x(t)]$ of the transient signal $x(t)$ were calculated. The envelope is

Table 1
Estimated data of the test system in Fig. 2(a).

	Mass (kg)*	Damping (Ns/m)		Linear stiffness (N/m)	Nonlinear stiffness (N/m^3)
Shaker and support	0.351	4.4		17,000	–
Vibration absorber	0.00755	0.12	Current Meth.	2380	5.93×10^{10}
			RSFM	2730	5.17×10^{10}

* Measured independently.

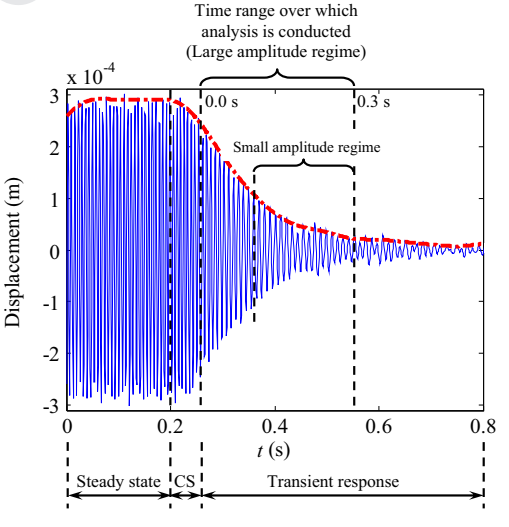

Fig. 3. Experimental results for the free vibration test. Solid line, measured time history response curves, dashed-dotted line, envelope obtained using Hilbert transform. CS, critical state which includes the transient effects of shaker switched-off.

Please cite this article as: B. Tang, et al., Experimental characterization of a nonlinear vibration absorber using free vibration, *Journal of Sound and Vibration* (2016), http://dx.doi.org/10.1016/j.jsv.2015.12.040

shown in Fig. 3. It should be noted that these parameters, which are estimated by using the Hilbert transform, are not accurate at the beginning and the end of the time history due to distortion induced by band-pass filtering the data [20]. Because some steady-state data was captured before the transient commenced, the distortion is restricted to the steady-state part and not the transient, (which is solely of interest here). Note that this distortion would have occurred in the transient part of the time history if an impact test had been carried out.

3. Model of the test set-up

To determine the system parameters from experimental data, a model of the vibration absorber and the shaker is required. Because of the way in which the test was set up, the appropriate model of the system is shown in Fig. 2(c), whose equation of motion is given by [27]

$$m_{\mathrm{EQ}}\ddot{x}+c\dot{x}+k_1x+k_3x^3=f(t) \tag{2}$$

where the overdots represent differentiation with respect to time, and $f(t)$ is the force generated by the shaker. Initially the force is harmonic $f(t)=F\cos(\omega t)$, where F is the amplitude of the force and ω is the angular forcing frequency, which is set to be just below the jump-down frequency. When the shaker is switched off, the vibration amplitude of the system decays away, with the frequency of vibration closely following the backbone curve [28].

The aim of the experiment was to determine the system parameters m_{EQ}, c, k_1, and k_3. These need to be determined from the measured time history shown in Fig. 3. Thus, an analytical solution to the free vibration of equation of motion, given in Eq. (2), with $f(t)=0$ is required. One way of doing this could be to apply standard perturbation techniques, which has been done by several authors, for example [28–32]. However the degree of nonlinearity in the experimental system was such that these techniques cannot provide a solution which replicates the experimental response for large amplitude excitation. This is further discussed in Section 5. The approach taken here, therefore, is based more on physical observation and results in a solution that is appropriate for a system with a high degree of stiffness nonlinearity and large initial amplitude of vibration, which is the case here. The consistency of the solution with those determined using perturbation techniques (which are given in Appendix A) is discussed in Section 5 for small amplitudes of vibration or weak cubic stiffness nonlinearity.

The general solution of Eq. (2) for $f(t)=0$ can be written as, for example [29]

$$x(t)=A(t)\cos[\phi(t)] \tag{3}$$

where $A(t)$ is the time dependent amplitude (or envelope) of the vibration and $\phi(t)$ is the time dependent phase. When the system undergoes free vibration and follows the backbone curve, the frequency of vibration changes as a function of time. As the system is hardening, this frequency, which is termed the time dependent (or instantaneous) damped natural frequency $\omega_d(t)$, reduces as the amplitude diminishes. The derivative of the time dependent phase is related to the time dependent damped natural frequency by $\dot{\phi}(t)=\omega_d(t)$ [19–20], which leads to

$$\phi(t)=\int_0^t \omega_d(\tau)\mathrm{d}\tau \tag{4}$$

For the system described by Eq. (2), the time dependent damped natural frequency (or the backbone curve) is given by [27]

$$\omega_d^2(t)=\omega_{dd}^2+\frac{3}{4}\frac{k_3}{m_{\mathrm{EQ}}}A^2(t) \tag{5}$$

where $\omega_{dd}=\omega_n\sqrt{1-\zeta^2}$ in which $\omega_n=\sqrt{k_1/m_{\mathrm{EQ}}}$ and $\zeta=c/(2\sqrt{m_{\mathrm{EQ}}k_1})$ are the undamped natural frequency and the damping ratio of the underlying linear system respectively. Now, if it assumed that the damping is light such that $\zeta<0.1$, and the effect of nonlinear stiffness is such that $A_0^2 3k_3/(8k_1)<<1$, in which A_0 is the initial amplitude of the mass, the decay of free vibration is approximately exponential (see Appendix A). The envelope of the time history can then be written as $A(t)=A_0e^{-\zeta\omega_n t}$. Substituting for this in Eq. (5) and combining this with Eq. (4) results in

$$\phi(t)\approx\sqrt{1-\zeta^2}\omega_n t+\frac{3}{16\zeta\sqrt{1-\zeta^2}}\frac{k_3}{k_1}A_0^2(1-e^{-2\zeta\omega_n t}), \tag{6}$$

so that Eq. (3) becomes

$$x(t)\approx A_0e^{-\zeta\omega_n t}\cos\left[\sqrt{1-\zeta^2}\omega_n t+\frac{3}{16\zeta\sqrt{1-\zeta^2}}\frac{k_3}{k_1}A_0^2(1-e^{-2\zeta\omega_n t})\right] \tag{7}$$

For the experimental test-rig, described in Section 2, it was found that Eq. (7) could only be used to describe the experimental response adequately when the initial amplitude was small. This is primarily because Eq. (7) assumes that the viscous damping results in an envelope that decays exponentially, but as shown by Burton [28] this is not the case when the amplitude of vibration or the stiffness nonlinearity is large. Any discrepancy in the envelope, however small, causes a discrepancy in the phase, which after several cycles of vibration, manifests itself as a large discrepancy due to an accumulation of phase error as time increases. If the initial amplitude is large, Eq. (5) can be used to determine the instantaneous

Please cite this article as: B. Tang, et al., Experimental characterization of a nonlinear vibration absorber using free vibration, *Journal of Sound and Vibration* (2016), http://dx.doi.org/10.1016/j.jsv.2015.12.040

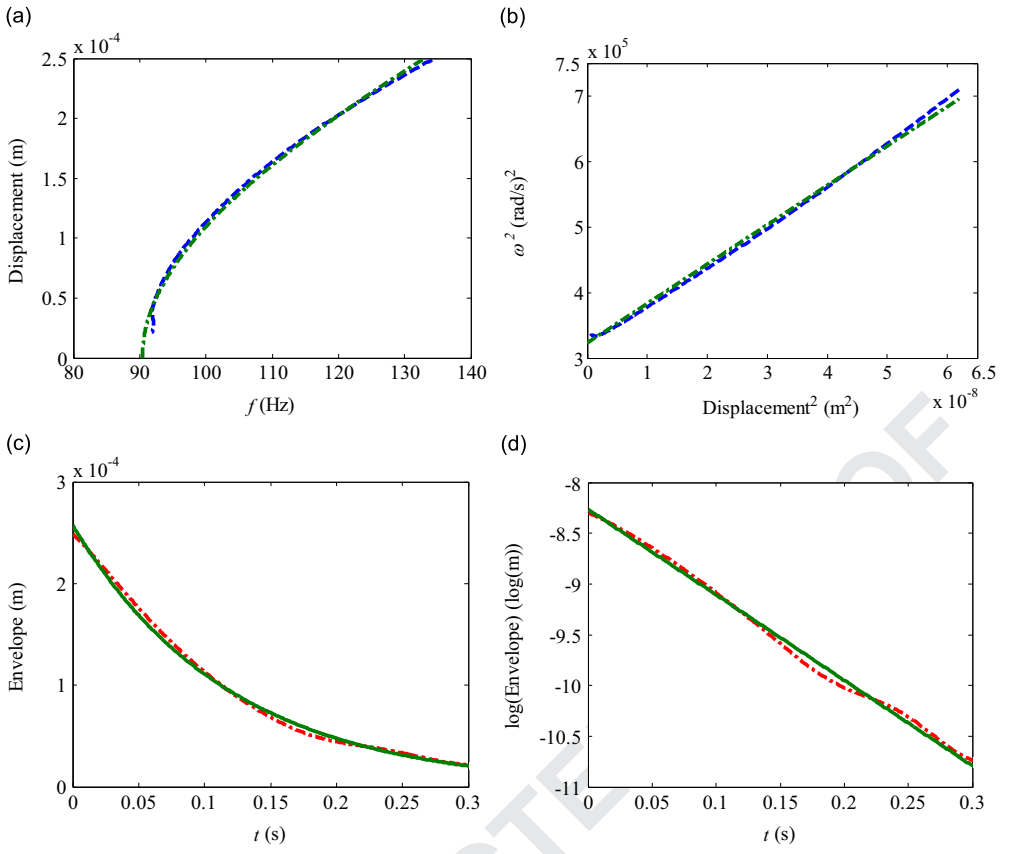

Fig. 4. The backbone and envelope of the experimental data. (a) ~~backbone curve,~~ (b) linear fit of backbone curve, (c) envelope, and (d) linear fit of envelope, ~~Dashed lines, measured backbone curve;~~ dashed-dotted line, envelope; solid line, fitting curves.

natural frequency using the measured envelope. This can be then combined with Eqs. (3) and (4) to reconstruct the free vibration of the mass.

Alternative expressions for the free vibration of the model of the system shown in Fig. 2(c) derived by using perturbation techniques, are given in Appendix A. Only first-order approximations are considered as these are most likely to result in the simple form of Eq. (7). It can be seen that the only method that can capture the behaviour of the system with low initial displacement and/or weak nonlinearity is the modified Krylov–Bogoliubov–Mitropolskiy method (MKBMM). This is probably because the assumed form of the solution can capture the phase of the response which changes exponentially as a function of time. None of the ~~first-order~~ perturbation methods leads to an expression which can capture the behaviour of the system for high initial amplitude, and for the degree of nonlinear stiffness studied experimentally in this paper.

4. Parameter estimation

The section of time history used for parameter estimation is indicated in Fig. 3. To estimate the time dependent damped natural frequency from experimental data the instantaneous phase needs to be determined from the time history. This is done by first integrating the captured acceleration signal twice with respect to time, and using the analytic signal given in Eq. (1). The time dependent phase is then unwrapped and the central difference method is used to determine the derivative with respect to time. Finally a low-pass filter is used to remove a small ripple, which is an artefact caused by the Hilbert transform [19,20].

A plot of the amplitude and the corresponding instantaneous damped natural frequency (the backbone curve) is shown in Fig. 4(a). Eq. (5) gives the theoretical relationship between these quantities. It can be seen that if the square of the frequency is plotted as a function of the square of the instantaneous amplitude then the result is a straight line with a slope of $3k_3/4m_{EQ}$ and the intersection of the frequency squared axis of $\omega_n^2(1-\zeta^2)$ [23]. This is plotted in Fig. 4(b) with the slope and the intersection calculated by fitting a straight line to the data, which is also shown in the figure. The estimated backbone curve is also shown in Fig. 4(a). It can be seen that Eq. (5) describes the backbone curve reasonably well.

To determine the nonlinear stiffness k_3, the mass m_{EQ} needs to be known. As mentioned previously this is given by $m_{EQ}=m_{shaker}m/(m_{shaker}+m)$. The mass m (which takes into account the accelerometer mass as well) was measured on a set

Please cite this article as: B. Tang, et al., Experimental characterization of a nonlinear vibration absorber using free vibration, *Journal of Sound and Vibration* (2016), http://dx.doi.org/10.1016/j.jsv.2015.12.040

of scales and was found to be 7.55 g; $m_{\text{shaker}} = 351$ g is the mass of the support structure, which was also measured using a set of scales, together with the moving mass of the shaker (230 g), which was obtained from the manufacturer specifications. Combining these masses gives an equivalent mass of $m_{\text{EQ}} = 7.39$ g. The brass plate, which has distributed mass of 2.7 g, between the clamped edge of the support structure and the absorber mass, which acts as the stiffness element in the absorber, has a negligible mass and is not considered in the lumped parameter model. From the estimate of the slope in Fig. 4b, the nonlinear stiffness was found to be $k_3 = 5.93 \times 10^{10}$ N/m^3, while from the intersection of the frequency squared axis, the damped natural frequency of the underlying linear system was estimated to be $\omega_{dd} = \omega_n\sqrt{1-\zeta^2} = 568.0$ rad/s (90.4 Hz).

The section of the envelope indicated in Fig. 3 is shown in Fig. 4(c) with the time set to zero at the start of the decay. The natural logarithm of the envelope is taken and this is plotted in Fig. 4(d). By fitting a straight-line to this plot the linear viscous damping ratio can be estimated by setting the slope of the graph to be equal to $\zeta\omega_n$. This was determined to be 8.42 rad/s, which results in a damping ratio (coefficient) of $\zeta \approx 0.015$ (0.12 Ns/m). The estimated envelope based on the assumption of linear viscous damping is overlaid in Fig. 4(c) and (d). It can be seen the envelope matches the exponential curve reasonably well. This suggests that the damping in the system is of the linear viscous or hysteretic type, as assumed initially. Finally, because the damping is very light, the undamped natural frequency is $\omega_n \approx \omega_{dd}$ and so the linear stiffness is given by $k_1 \approx \omega_{dd}^2 m_{\text{EQ}} = 2380$ N/m. The identified parameters are given in Table 1. In particular, the identified linear and cubic stiffness coefficients are in agreement with the approximate nominal values of 2530 N/m and 4.98×10^{10} N/m^3 respectively, obtained analytically by considering the static relationship between the applied static force at the centre of the circular plate and the deflection at that point [33], for a Poisson's ratio of 0.3 and a Young's modulus of 110 GPa.

As a check on the estimated stiffness parameters, they were also identified using the Restoring Force Surface (RFS) Method [26]. To apply this method, the equation of motion given in Eq. (2) is written with the force $f(t) = 0$ to give

$$c\dot{x} + k_1 x + k_3 x^3 = -m_{\text{EQ}}\ddot{x} \tag{8}$$

The right-hand side of Eq. (8) is known, as the acceleration and mass are measured. The velocity and the displacement are determined by time-domain integration of the acceleration signal. A three-dimensional surface $(x, \dot{x}, m_{\text{EQ}}\ddot{x})$ can then be plotted using the data at each measured time instant. A section through the surface was then extracted between the values of -0.1 m/s $< \dot{x} <$ 0.1 m/s. This is plotted in Fig. 5 as the stiffness force. A polynomial was subsequently fitted to the data to give the linear and nonlinear stiffness which are $k_1 = 2730$ N/m and $k_3 = 5.17 \times 10^{10}$ N/m^3. These are also given in Table 1, and compare reasonably well with those determined by the method described in this paper. Comparing the linear and nonlinear stiffness results obtained using the current method and RFS method, the differences are both about 13%. The reconstructed spring restoring curves with the stiffness parameters obtained using the two methods, which are given in Table 1, are also plotted in Fig. 5, and compared well with each other. Using the estimated parameters given in Table 1, the time history response reconstructed from current method is compared with actual response in the next section.

5. Discussion

To determine whether the identification procedure is successful, a reconstructed time history of the transient response is compared with the measured vibration for a large and a small initial amplitude of vibration as shown in Fig. 3. For a large initial amplitude (after the CS period), Eqs. (3)–(5) are used, together with the measured envelope. The instantaneous phase is therefore determined by carrying out the integration in Eq. (4) numerically, with the parameters given in Table 1. The results are shown in Fig. 6(a). It can be seen that there is a very good reconstruction of the time history, which matches well with the measured data. Note that in this figure $t = 0$ corresponds to $t = 0.254$ s in Fig. 3. For a small initial amplitude marked

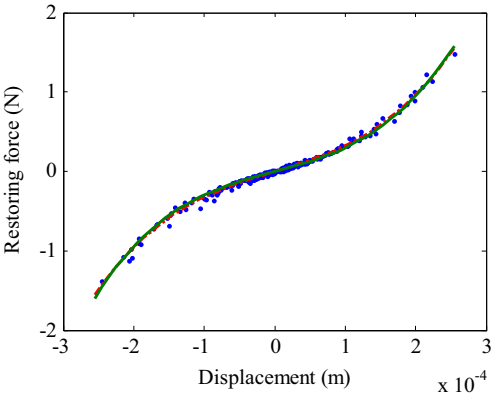

Q3 **Fig. 5.** Estimated stiffness force from the measured data using the RFSM. Dashed red line, least square fit to RFSM data; solid green line, current method. (For interpretation of the references to colour in this figure legend, the reader is referred to the web version of this article.)

Please cite this article as: B. Tang, et al., Experimental characterization of a nonlinear vibration absorber using free vibration, *Journal of Sound and Vibration* (2016), http://dx.doi.org/10.1016/j.jsv.2015.12.040

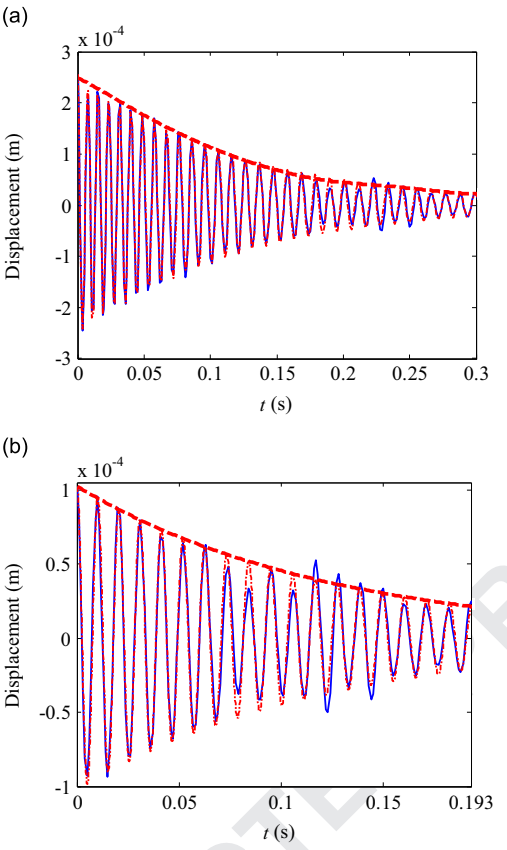

Fig. 6. Experimental and reconstructed time history for (a) large initial displacement, calculated using the actual envelope and (b) small initial displacement, calculated using Eq. (7). Thick dashed lines, envelope; thin solid lines, experimental results; dashed-dotted lines, reconstructed curve.

in Fig. 3, Eq. (7) is used to reconstruct the time response with the parameters given in Table 1. The results are shown in Fig. 6 (b). It can be seen that the reconstructed time history matches well with the measured data. Note that in this figure $t=0$ corresponds to $t=0.36$ s in Fig. 3.

It should be noted that a very accurate prediction of the instantaneous damped natural frequency is required for an accurate prediction of the instantaneous phase over the duration of the time history. As the instantaneous amplitude affects the instantaneous frequency, an accurate estimate of this is required. This is the principal reason why the expression for the response given in Eq. (7) does not result in a time history that matches the experimental result well for a large initial amplitude.

To compare the precision of the closed-form solution given by Eq. (7), the free response of the system, plotted using the non-dimensional form of this equation given by Eq. (A.3), is compared with the numerical solution of the non-dimensional equation of motion given by Eq. (A.1) for different values of damping ratio ζ and nonlinearity γ. In the non-dimensional form γ includes both the effects of nonlinear stiffness k_3 and initial displacement A_0. The root mean square error (RMSE) between the two time histories, given by [26]

$$\mathrm{RMSE}(y)=\sqrt{\frac{\sum_{i=1}^{N}(y_i-\hat{y}_i)^2}{N\sigma_{\hat{y}}^2}} \tag{9}$$

is calculated, where y_i and $\hat{y}_i$ are the response amplitudes of the analytical and numerical solutions at each time step respectively, N is the number of sample points, and $\sigma_{\hat{y}}^2$ is the mean square value of the numerical solution.

The RMSE given by Eq. (9) includes both the error in the amplitude and phase of the analytical solution, and can ~~give~~ be used to give a comparison of the solutions at different values of nonlinearity γ and damping ratio ζ. Note that if the analytical result is zero for all time then the RMSE would be unity. Eq. (9) is plotted in Fig. 7. It can be seen that for $\gamma<0.1$ and $\zeta<0.1$ the analytical solution is quite accurate, with the RSME <0.1.

The corresponding non-dimensional parameters for the time histories with large and small initial displacements, which are plotted in Fig. 6(a,b), are given in Table 2 and are also shown in Fig. 7, as a square and a circle, respectively. The damping ratio of the nonlinear absorber is $\zeta=0.015$, and the nonlinear parameter for the large initial amplitude case is $\gamma\approx1.63$, so

Please cite this article as: B. Tang, et al., Experimental characterization of a nonlinear vibration absorber using free vibration, *Journal of Sound and Vibration* (2016), http://dx.doi.org/10.1016/j.jsv.2015.12.040

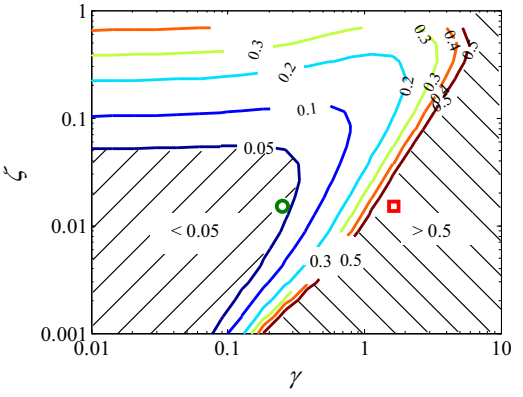

Fig. 7. Contour plot showing the root mean square error (RMSE) between the approximate solution (Eq. (7)) and the numerical solution. □, Nonlinear system with $\gamma = 1.63$, $\zeta = 0.015$; ○, nonlinear system with $\gamma = 0.25$, $\zeta = 0.015$.

Table 2
Estimated non-dimensional data of the test system in Fig. 2(a).

Initial displacement (mm)	Damping ratio ζ	Nonlinearity γ
0.256	0.015	1.63
0.1	0.015	0.25

that the RMSE > 0.5, whereas for the small initial amplitude case $\gamma \approx 0.25$ so that the RMSE < 0.05. This demonstrates why the analytical solution is appropriate for the small initial amplitude case, but not for the large initial amplitude case in the experiments.

6. Conclusions

This paper has shown how the system parameters of a nonlinear vibration absorber can be determined experimentally from a free vibration test. The method involved the excitation of the nonlinear absorber by an electrodynamic shaker such that the system was close to its jump-down frequency, where the shaker was working in its mass controlled regime, and then the source signal was switched-off. The system then vibrated freely, and the vibration of the absorber mass was sampled and used in the characterization process. Using the Hilbert transform the instantaneous envelope and instantaneous damped natural frequency were estimated from the free vibration signal. Subsequently, the damping and stiffness parameters were determined from this data, while the mass of the system was simply measured using a weighing scale. The results were compared with the RFS method and it was found that they differenced by only about 13%. Using the estimated parameters, the time history of the absorber mass was reconstructed and compared with the measured data for high and low initial amplitudes of excitation. The results are considered to be good. Further, an analytical expression was determined using the backbone curve together with the assumption of an exponential decay of the free vibration. This was found to estimate the response of the measured system well for low initial level of excitation, but not for a high initial level of vibration. The expression is found to be only appropriate if the nonlinearity is small or if both the nonlinearity and the damping are high.

Acknowledgements

Q4 The first author wishes to acknowledge the financial support from National Natural Science Foundation of China (Grant no. 11202048), the Fundamental Research Funds for the Central Universities of China (Grant no. DUT15QY30), and CNPq (Grant no. 401360/2012-1), which enabled him to finish this paper in UNESP, Brazil. The second and third authors wish to acknowledge the support of the FAPESP.

Appendix A. Analytical solutions determined using ~~first-order~~ perturbation methods

In this appendix the expression for free vibration which was derived in Eq. (7) based on physical arguments, is compared with three solutions to the equation of motion determined using three conventional ~~first-order~~ perturbation approaches.

Please cite this article as: B. Tang, et al., Experimental characterization of a nonlinear vibration absorber using free vibration, *Journal of Sound and Vibration* (2016), http://dx.doi.org/10.1016/j.jsv.2015.12.040

These are the method of multiple-scales (MMS) [30], Lindstedt–Poincaré method (LPM) [31], and the modified Krylov–Bogoliubov–Mitropolskiy (KBM) method [32]. Non-dimensional equations are used in the comparison.

First, consider Eq. (2) with $f(t)=0$ written in non-dimensional form as

$$y''+2\zeta y'+y+\gamma y^3=0 \tag{A.1}$$

where $y=x/A_0, \gamma=k_3A_0^2/k_1, \zeta=c/2m_{EQ}\omega_n$, $\omega_n=\sqrt{k_1/m_{EQ}}$, $\tau=\omega_n t$, $A_0=x(0)$ is the initial displacement of the mass, with initial conditions $y(0)=1, y'(0)=0$. The solution to Eq. (A.1) is [29]

$$y(\tau)=A(\tau)\cos[\phi(\tau)] \tag{A.2}$$

where $A(\tau)$ is the non-dimensional envelope and $\phi(\tau)$ is the phase which is dependent on non-dimensional time. This is related the non-dimensional damped natural frequency, $\phi(\tau)=\int_0^\tau \Omega(\tau)d\tau$, in which $\Omega(\tau)=\omega(\tau)/\omega_n$. Eq. (7), which was determined using the backbone curve can be written in non-dimensional form as the solution to Eq. (A.1), and is given by

$$y(\tau)\approx e^{-\zeta\tau}\cos\left[\Omega_d\tau+\frac{3\gamma}{16\Omega_d\zeta}(1-e^{-2\zeta\tau})\right] \tag{A.3}$$

where $\Omega_d=\sqrt{1-\zeta^2}$ is the non-dimensional linear damped natural frequency of the system.

If the damping is small such that $\zeta=O(\gamma)$, the MMS [30] can be used in a straightforward manner to obtain a *first order* approximate solution. The details of the solution procedure are not given here, but can be found in [30]. The result is

$$y(\tau)=e^{-\zeta\tau}\cos\left[\tau+\frac{3\gamma}{16\zeta}(1-e^{-2\zeta\tau})\right] \tag{A.4}$$

Comparing this with Eq. (A.3), it can be seen that the two results are similar, especially if the damping is small. However, if the damping is not small then they will give different results. It can also be seen, that although the nonlinearity has a similar effect on the time dependent phase (and hence frequency), if the nonlinearity is set to zero, the result given by Eq. (A.4) does not give the case for the damped linear system, whereas the result given by Eq. (A.3) does.

Another method considered is the Lindstedt–Poincaré method (LPM) [31]. A new time variable $\tau=s(1+\gamma\Omega_1+\gamma^2\Omega_2+\cdots)$ is introduced, together with the zero and first order terms of the approximate solution $y=y_0(s)+\gamma y_1(s)+\gamma^2y_2(s)+\cdots$. When convolution [31] is used to solve the system of equations, the *first order* solution is obtained as

$$y(\tau)\approx e^{-\zeta\tau}\cos\left[\left(\Omega_d+\frac{3\gamma}{8\Omega_d}\right)\tau\right] \tag{A.5}$$

It can be seen from Eq. (A.5) that the envelope is the same as that for the response given by Eq. (A.3), but the phase and hence the damped natural frequency is predicted to be independent of frequency. Hence, Eq. (A.5) does not give an adequate description of the response. It should be noted that Eq. (A.5) can be derived from Eq. (A.3), by assuming that $2\zeta\tau<<1$ so that $e^{-2\zeta\tau}\approx 1-2\zeta\tau$. The effect of making this substitution, however, is to remove the time dependency of the damped natural frequency, which is clearly incorrect.

The final method which can be used to obtain the solution to Eq. (A.1) is the Modified KBM Method (MKBMM) [32]. The solution is assumed to be of the form $y(a,\psi)$, where a and ψ are functions of τ, and y is periodic in ψ. For the first order approximate solution, the solution is assumed to be of the form $y=a(\tau)\cos[\psi(\tau)]$. The time differentials of a and ψ are ξ and Ω respectively. To solve Eq. (A.1), these variables are substituted into this equation, and together with y, they are expanded as a power series of the non-dimensional nonlinear stiffness γ, so that $y=y_0+\gamma y_1+\cdots$, $\xi=-\zeta a+\gamma\xi_1+\cdots$, $\Omega=\Omega_d+\gamma\Omega_1+\cdots$. Considering only the zero and first order terms of γ, a system equation is obtained. The nonlinear term γy_0^3 is expanded as a Fourier series, and ξ_1 and Ω_1 are expanded as a power series. By omitting the secular terms, ξ_1 and Ω_1 are obtained. When y_1 is expanded as a Fourier series and the harmonic balance method is used, the approximate first order results are obtained. Applying the initial conditions results in [32]

$$y(\tau)\approx\frac{e^{-\zeta\tau}}{\left(1+\frac{3\gamma(e^{-2\zeta\tau}-1)}{8}\right)^{1/2}}\cos\left[\Omega_d\tau-\frac{\Omega_d}{2\zeta}\ln\left(1+\frac{3\gamma(e^{-2\zeta\tau}-1)}{8\Omega_d^2}\right)\right] \tag{A.6}$$

Examining Eq. (A.6), it can be seen that the damped natural frequency and the envelope are both predicted to be dependent on the nonlinearity. If it is assumed that $3\gamma(e^{-2\zeta\tau}-1)/8\ll 1$ and $\Omega_d^2\approx 1$, then the Eq. (A.6) reduces to Eq. (A.3). As $\gamma\to 0$ Eq. (A.6) reduces to the response of a linear damped oscillator, and is thus a consistent model, and is also valid for high values of damping.

References

[1] H. Frahm, Device for damping vibrations of bodies, Patent No. 989, 958, 1911.

[2] J. Ormondroyd, J.P. Den Hartog, The theory of the dynamic vibration absorber, *Transactions of the American Society of Mechanical Engineers* 50 (1928) 9–22.

[3] J.Q. Sun, M.R. Jolly, M.A. Norris, Passive, adaptive and active tuned vibration absorbers – a survey, *Transactions of the ASME, Journal of Mechanical Design* 117 (B) (1995) 234–242.

Please cite this article as: B. Tang, et al., Experimental characterization of a nonlinear vibration absorber using free vibration, *Journal of Sound and Vibration* (2016), http://dx.doi.org/10.1016/j.jsv.2015.12.040

[4] S.S. Oueini, A.H. Nayfeh, J.R. Pratt, A review of development and implementation of an active nonlinear vibration absorber, *Archive of Applied Mechanics* 69 (8) (1999) 585–620.
[5] M.J. Brennan, Some recent developments in adaptive tuned vibration absorbers/neutralisers, *Shock and Vibration* 13 (4–5) (2006) 531–543.
[6] L. Kela, P. Vähäoja, Recent studies of adaptive tuned vibration absorbers/neutralizers, *Transactions of the ASME, Applied Mechanics Reviews* 62 (6) (2009) 060801.
[7] R.E. Roberson, Synthesis of a nonlinear dynamic vibration absorber, *Journal of the Franklin Institute* 254 (3) (1952) 205–220.
[8] S.F. Masri, Theory of the dynamic vibration neutralizer with motion-limiting stops, *Transactions of ASME, Journal of Applied Mechanics* 39 (2) (1972) 563–568.
[9] R. Riganti, Subharmonic steady vibrations of a nonlinear damper with two degrees of freedom and viscous damping, *International Journal of Nonlinear Mechanics* 15 (3) (1980) 173–183.
[10] H.J. Rice, Combinational instability of the nonlinear vibration absorber, *Journal of Sound and Vibration* 108 (3) (1986) 526–532.
[11] I.N. Jordanov, B.I. Cheshankov, Optimal design of linear and non-linear dynamic vibration absorbers, *Journal of Sound and Vibration* 123 (1) (1988) 157–170.
[12] H.J. Rice, J.R. McCraith, Practical non-linear vibration absorber design, *Journal of Sound and Vibration* 116 (3) (1987) 545–559.
[13] S. Natsiavas, Steady state oscillations and stability of non-linear dynamic vibration absorbers, *Journal of Sound and Vibration* 156 (2) (1992) 227–245.
[14] S.J. Zhu, Y.F. Zheng, Y.M. Fu, Analysis of non-linear dynamics of a two-degree-of-freedom vibration system with non-linear damping and non-linear spring, *Journal of Sound and Vibration*271 (1–2) (2004) 15–24.
[15] A.F. Vakakis, O.V. Gendelman, L.A. Bergman, D.M. McFarland, G. Kerschen, Y.S. Lee, *Nonlinear Targeted Energy Transfer in Mechanical and Structural Systems*, Springer, Dordrecht, 2008.
[16] R. Viguié, G. Kerschen, Nonlinear vibration absorber coupled to a nonlinear primary system: A tuning methodology, *Journal of Sound and Vibration* 326 (3–5) (2009) 780–793.
[17] M.J. Brennan, G. Gatti, The characteristics of a nonlinear vibration neutralizer, *Journal of Sound and Vibration* 331 (13) (2012) 3158–3171.
[18] G. Kerschen, K. Worden, A.F. Vakakis, J.C. Golinval, Past, present and future of nonlinear system identification in structural dynamics, *Mechanical Systems and Signal Processing* 20 (3) (2006) 505–592.
[19] M. Feldman, Non-linear system vibration analysis using Hilbert transform-I. Free vibration analysis method 'FREEVIB', *Mechanical Systems and Signal Processing* 8 (2) (1994) 119–127.
[20] M. Feldman, *Hilbert Transform Applications in Mechanical Vibration*, Wiley, Chichester, 2011.
[21] G.C. Kung, Y.H. Pao, Nonlinear flexural vibrations of a clamped circular plate, *Transactions of the ASME, Journal of Applied Mechanics* 39 (4) (1972) 1050–1054.
[22] W.J. Parzygnat, Y.H. Pao, Resonance phenomena in the nonlinear vibration of plates governed by Duffing's equation, *International Journal of Engineering Science* 16 (12) (1978) 999–1017.
[23] Y. Benhafsi, J.E.T. Penny, M.I. Friswell, A parameter identification method for discrete nonlinear systems incorporating cubic stiffness elements, *The International Journal of Analytical and Experimental Modal Analysis* 7 (3) (1992) 179–195.
[24] B. Tang, M.J. Brennan, V. Lopes Jr., S. da Silva, R. Ramlan, Using nonlinear jumps to estimate cubic stiffness nonlinearity: an experimental study, Proceedings of the Institution of Mechanical Engineers, Part C: Journal of Mechanical Engineering Science, doi:10.1177/0954406215606746 (OnlineFirst), first published on September 16, 2015.
[25] Y.S. Hsu, *The Performance of a Nonlinear Vibration Absorber*, University of Southampton, Southampton, UK, 2014.
[26] K. Worden, G.R. Tomlinson, *Nonlinearity in Structural Dynamics: Detection, Identification and Modelling*, Institute of Physics Publishing, Bristol and Philadelphia, 2001.
[27] I. Kovacic, M.J. Brennan, *The Duffing Equation: Nonlinear Oscillators and their Behaviour*, Wiley, Chichester, 2011.
[28] T.D. Burton, On the amplitude decay of strongly non-linear damped oscillators, *Journal of Sound and Vibration* 87 (4) (1983) 535–541.
[29] Y.A. Mitropol'skii, Problems of the asymptotic theory of nonstationary vibrations, Israel Program for Scientific Translations, Jerusalem, 1965.
[30] A.H. Nayfeh, D.T. Mook, *Nonlinear Oscillations*, Wiley, New York, 1995.
[31] R.G. White, Effects of non-linearity due to large deflections in the derivation of frequency response data from the impulse response of structures, *Journal of Sound and Vibration* 29 (3) (1973) 295–307.
[32] K.S. Mendelson, Perturbation theory for damped nonlinear oscillations, *Journal of Mathematical Physics* 11 (12) (1970) 3413–3415.
[33] S. Timoshenko, S. Woinowsky-Krieger, *Theory of Plates and Shells*, McGraw-Hill, New York, 1959, 412–416.

Please cite this article as: B. Tang, et al., Experimental characterization of a nonlinear vibration absorber using free vibration, *Journal of Sound and Vibration* (2016), http://dx.doi.org/10.1016/j.jsv.2015.12.040